

Manuscript Number: FUSENGDES-D-18-00235R1

Title: A Review of Impact Properties of Tungsten Materials

Article Type: Full Length Article

Keywords: Tungsten, Charpy impact property, Powder metallurgy, Rolling, Forging, Swaging, Dispersion strengthening, Solid solution, Grain refining, Hall-Petch law

Corresponding Author: Dr. Shuhei Nogami,

Corresponding Author's Institution: Tohoku University

First Author: Shuhei Nogami

Order of Authors: Shuhei Nogami; Shotaro Watanabe; Jens Reiser; Michael Rieth; Sven Sickinger; Akira Hasegawa

Abstract: One of the most critical issues affecting tungsten (W) as plasma facing material is ductile-to-brittle transition behavior. It is well known that the microstructure of W materials is influenced by the fabrication methods and histories, which can affect those behaviors. In this paper, the current status of Charpy impact properties (ductile-to-brittle transition temperature (DBTT) etc.) of pure and modified W materials fabricated by several methods and histories are reviewed based on the open literatures and the possibility of integrated interpretation of Charpy impact properties of W materials from different production routes is discussed.

Corresponding Author

Name Shuhei Nogami

Postal address Department of Quantum Science and Energy Engineering, Graduate School
of Engineering, Tohoku University, 6-6-01-2, Aramaki-aza-Aoba, Aoba-ku,
Sendai 980-8579, Japan

Telephone +81-22-795-7923

Fax number +81-22-795-7924

E-mail address shuhei.nogami@qse.tohoku.ac.jp

Response to Reviewers

I really appreciate your kind and quick reviews. We hope that our researches contribute fusion divertor design and operation. Thank you very much again.

Highlight

- (1) The Charpy impact properties of W materials are dependent on the fabrication methods and histories even if their major chemical composition is the same.
- (2) It is possible that the DBTT and USE of pure W could be integratedly understood using Hall-Petch type relations even if materials are from different production routes.

A Review of Impact Properties of Tungsten Materials

Shuhei Nogami¹, Shotaro Watanabe², Jens Reiser³, Michael Rieth⁴, Sven Sickinger⁵,
Akira Hasegawa⁶

¹ Department of Quantum Science and Energy Engineering, Graduate School of Engineering, Tohoku University, 6-6-01-2, Aramaki-aza-Aoba, Aoba-ku, Sendai 980-8579, Japan, shuhei.nogami@qse.tohoku.ac.jp

² Department of Quantum Science and Energy Engineering, Graduate School of Engineering, Tohoku University, 6-6-01-2, Aramaki-aza-Aoba, Aoba-ku, Sendai 980-8579, Japan, shotaro.watanabe.s5@dc.tohoku.ac.jp

³ Institute for Applied Materials, Karlsruhe Institute of Technology, Hermann-von-Helmholtz-Platz 1, 76344 Eggenstein-Leopoldshafen, Germany, jens.reiser@kit.edu

⁴ Institute for Applied Materials, Karlsruhe Institute of Technology, Hermann-von-Helmholtz-Platz 1, 76344 Eggenstein-Leopoldshafen, Germany, michael.rieth@kit.edu

⁵ Institute for Applied Materials, Karlsruhe Institute of Technology, Hermann-von-Helmholtz-Platz 1, 76344 Eggenstein-Leopoldshafen, Germany, sven.sickinger@kit.edu

⁶ Department of Quantum Science and Energy Engineering, Graduate School of Engineering, Tohoku University, 6-6-01-2, Aramaki-aza-Aoba, Aoba-ku, Sendai 980-8579, Japan, akira.hasegawa@qse.tohoku.ac.jp

A Review of Impact Properties of Tungsten Materials

Shuhei Nogami¹, Shotaro Watanabe¹, Jens Reiser², Michael Rieth², Sven Sickinger²,
Akira Hasegawa¹

¹ Department of Quantum Science and Energy Engineering, Graduate School of Engineering, Tohoku University, 6-6-01-2, Aramaki-aza-Aoba, Aoba-ku, Sendai 980-8579, Japan

² Institute for Applied Materials, Karlsruhe Institute of Technology, Hermann-von-Helmholtz-Platz 1, 76344 Eggenstein-Leopoldshafen, Germany

Abstract

One of the most critical issues affecting tungsten (W) as plasma facing material is ductile-to-brittle transition behavior. It is well known that the microstructure of W materials is influenced by the fabrication methods and histories, which can affect those behaviors. In this paper, the current status of Charpy impact properties (ductile-to-brittle transition temperature (DBTT) etc.) of pure and modified W materials fabricated by several methods and histories are reviewed based on the open literatures and the possibility of integrated interpretation of Charpy impact properties of W materials from different production routes is discussed.

Keywords:

Tungsten, Charpy impact property, Powder metallurgy, Rolling, Forging, Swaging, Dispersion strengthening, Solid solution, Grain refining, Hall-Petch law

1. Introduction

Plasma facing components (PFCs) of fusion reactors, such as divertor and blanket, are subjected to high heat flux (HHF) loading during operation. To protect these components from HHF loading from a few to 20 MW/m², plasma facing material (PFM) is applied to the surface of PFCs [1]. Tungsten (W) is a primary candidate of the PFM because of its high melting point, thermal conductivity, sputtering resistance, and low tritium retention [2]. However, improvement of thermo-mechanical properties of W materials are still required to overcome the potential disadvantages of W materials, and then to provide an additional margin of safety, reliability, and lifetime of PFCs. The most critical issues affecting the thermo-mechanical properties of W materials are ductile-to-brittle transition [3–11] and recrystallization [12–15]. Most of W materials show the ductile-to-brittle transition above room temperature (low temperature brittleness of as-fabricated materials) and show brittleness after recrystallization at elevated temperature (embrittlement caused by recrystallization). Therefore, low temperature brittleness and recrystallization embrittlement should be suppressed in W materials, which can limit the operation temperature of PFCs.

It is well known that the as-fabricated microstructure of W materials and its recovery and recrystallization behaviors under elevated temperatures are strongly influenced by the fabrication methods and histories. Furthermore, microstructural anisotropy cannot be negligible in worked W materials (i.e., rolled plates and swaged rods) [16–20]. Therefore, the microstructure and its anisotropy induced by individual fabrication methods and histories should be taken into account in W materials even if their major chemical composition is the same.

Although the ductile-to-brittle transition temperature (DBTT), which strongly depends on the testing method, cannot be directly used as a parameter for structural design and operation, it has been utilized for evaluation of the ductile-to-brittle transition behavior of

structural materials and for systematic screening studies of them. The Charpy impact testing is one of the most available and widespread techniques to evaluate the DBTT. In the case of W materials, data of DBTT has been limited because there are very few Charpy impact testing machine with a high temperature vacuum furnace, which can evaluate the DBTT above room temperature with suppression of environmental effects (e.g., oxidation effect). Therefore, systematic interpretation of the effects of microstructural and compositional modifications (e.g., grain-refining, alloying, and dispersion-strengthening) is currently not enough.

This paper reviews the current status of the Charpy impact properties of W materials developed for the PFM applications, including pure and modified ones fabricated by several methods and histories, based on the open literatures during recent ten years, and then discuss for the integrated interpretation of Charpy impact properties of W materials from different production routes. All the data shown in this paper are obtained using a Charpy impact testing machine with a high temperature vacuum furnace of the Institute of Applied Materials (IAM), Karlsruhe Institute of Technology (KIT), Germany [21]. Most of the data, which are those of W materials from European communities for the PFM applications, have already been published in several papers [21–26] and some data, which are those of W materials from Tohoku university, Japan, also for the PFM applications are newly obtained for this paper.

2. Current status of Charpy impact properties

2.1 Hot-rolled plates

Among W materials, plate fabricated by powder metallurgy and rolling is one of the key forms for the PFM applications. In the current design of ITER full W monoblock divertor target, hot-rolled pure W plate is a leading candidate material [27]. Fig. 1 (a) shows the Charpy impact properties of as-received hot-rolled plates with 4 mm thickness made of pure

W and W materials, which are dispersion-strengthened by potassium (K) bubbles (K-doped W) and by lanthanum oxide (La_2O_3) particles (W-1% La_2O_3) [21–25]. Specimen and methods of the instrumented Charpy impact testing in this section is the same as those described in the section 3.2. The nomenclature of the directions of hot-rolled W plates and specimens is shown in Fig. 2 (a). The L direction correspond to the rolling direction of the plate. The first letter of the L-S etc. indicates the direction perpendicular to the expected crack plane while the second letter stands for the expected direction of crack growth.

As shown in Fig. 1 (a), significant difference of upper shelf energy (USE) of hot-rolled pure W plates among the L-S, L-T, and T-L directions are observed. Although the DBTT along T-L direction is not clarified, the effect of test direction on the DBTT of pure W will not be also small. In general, the impact properties along L-S and T-L directions are the best and the worst among them, respectively. These anisotropies of the impact property could be attributed to the as-fabricated microstructure and its anisotropy [16–20].

Grain refining [28], work hardening [29], solid solution alloying [30, 31], and dispersion strengthening [31] are known as conventional methods to improve the mechanical properties of W materials. The K-doping is one of the dispersion strengthening methods [32–34]. K-doped W contains nano bubbles filled with K, which are mainly dispersed at the grain boundaries [35]. The K-bubbles hinder the motion of grain boundaries and dislocations, leading to higher strength at high temperatures and suppression of recrystallization. Dispersion strengthening by nano particles by oxide and carbide such as La_2O_3 and titanium carbide (TiC) is another well-known method not only for W materials but for the other metals [36–38]. Although the optimization of these oxide/carbide dispersion strengthened W materials is not so easy, some materials showed excellent mechanical properties [38].

As shown in Fig. 1 (a), the dispersion of K bubbles and La_2O_3 particles showed no significant positive effects on impact properties of hot-rolled W plates below 1000 °C. In

principle, their effects on mechanical properties are expected especially at higher temperature. For example, the K-doping is originally developed to suppress creep deformation caused by grain boundary sliding of W. Therefore, no effects of dispersion of K bubbles and La_2O_3 particles on impact properties could be detected because of relatively low test temperatures.

However, grain refining, which can generally improve the strength, is achieved by the K-doping without any heavy rolling [20, 39–42]. As a consequence, the different K-doped W plates from those in Fig. 1 (a) showed the improvement of tensile strength below 1000 °C in comparison with the pure W plates, which could be attributed to the K-doping [18, 20, 39, 41, 42]. Therefore, it is necessary to further investigate the effect of K-doping and La_2O_3 particles dispersion in hot-rolled W plates based on the microstructural viewpoints.

2.2 Forged round-blanks

Round-blanks of W materials fabricated by powder metallurgy and forging were developed for the PFM applications, especially by European community. Fig. 1 (b) shows the Charpy impact properties of as-received round-blanks with 175 mm diameter and 29 mm thickness made of pure W and W alloyed by tantalum (Ta), molybdenum (Mo), and vanadium (V) [24, 26]. Specimen and methods of the testing in this section is the same as those described in the section 3.2. The nomenclature of the directions of forged W round-blanks and specimens is shown in Fig. 2 (b). The L direction correspond to the radial direction of the round-blanks. The first and the second letters of the L-S etc. indicate the same meanings as the hot-rolled plate.

The round-blank of pure W shows smaller difference of the USE and DBTT between the L-S and L-T directions than the hot-rolled plate of pure W. In the case along L-S direction, the USE and DBTT of round-blank of pure W are lower and higher than the hot-rolled plate of pure W, respectively. In the case along S-L direction, the round-blank of pure W shows

brittle impact properties with no DBTT at all temperatures below 1000 °C.

Solid solution alloying is very common to improve the properties of W materials including impact properties, strength, ductility, and recrystallization resistance [18, 30, 31, 41]. As shown in Fig. 1 (b), the alloying by 1%Ta and 50%Mo in W round-blanks shows no or very small positive effects on impact properties below 1000 °C, which is dependent on the test temperature, although the big scatter of absorbed energy is observed in the W-1%Ta. In contrast, the degradation of impact properties is caused due to the alloying by 5%Ta, 20%Mo, and 5%V. In these cases, brittle impact properties with no DBTT at all temperatures below 1000 °C are observed, which are similar to those observed in the round-blank of pure W along S-L direction.

Rhenium (Re) and iridium (Ir) are known as solid solution alloying element to improve ductility, strength, and recrystallization resistance of W materials, which are caused by the difference in the electronic structure [18, 30, 31, 41, 43–46]. Therefore, the effects of alloying by Re and Ir on the impact properties of W materials are expected to be clarified in future although there is a cost issue in these elements.

2.3 Swaged rods

Among W materials, rod fabricated by powder metallurgy and swaging is also one of the key forms for the PFM applications. In the current design of ITER full W monoblock divertor target, swaged pure W rod is another leading candidate material [27]. W narrow rods and wires have been widely explored as filament etc., however, limited data is available on bulk W rods for the PFM applications [20, 46–48]. Fig. 1 (c) shows the Charpy impact properties of as-received swaged rods with different diameters made of pure W, K-doped W, W-1%La₂O₃, and W-1%Re-1%La₂O₃ [21, 24–26]. Specimen and methods of the testing in this section is the same as those described in the section 3.2. The nomenclature of the

directions of swaged W rods and specimens is shown in Fig. 2 (c). The L direction correspond to the axial direction of the rods. The first and the second letters of the L-S etc. indicate the same meanings as the hot-rolled plate and forged round-blank.

The USE of the pure W rods is the highest among three pure W forms (plate, round-blank, and rod). Fractography of specimens after the impact tests points out that the delamination fracture along L direction is observed in the pure W plate and round-blank specimens along L-S direction above DBTT to 1000 °C, while the pure W rod specimens along L-R direction showed the delamination fracture above DBTT to 800 °C and the ductile fracture above 800 °C to 1000 °C [21, 24, 26]. Due to this difference in the fracture manner, very high USE could be obtained in the pure W rod.

In case of the W rods with 6.9 mm diameter, the K-doping and La₂O₃ particles dispersion decreased the DBTT by 50–100 °C in comparison with the pure W. In contrast, decrease in USE above 800 °C occurred due to the K-doping and La₂O₃ particles dispersion. According to the fractography of these materials [21, 24, 26], the K-doped W and W-1%La₂O₃ show the delamination fracture from DBTT to 1000 °C and show no ductile fracture, which is observed in the pure W above 800 °C. Therefore, decrease in the USE is caused by the suppression of the ductile fracture at higher temperature conditions.

The decrease in diameter of rods, which corresponds to the increase in the reduction ratio along the radial direction of rods in the swaging process, is effective to improve the impact properties. In case of the pure W and W-1%La₂O₃, the DBTT shifted to lower temperatures by approximately 100 °C due to the decrease in the diameter from 20 mm to 6.9 mm. It is known that the strength and ductility of swaged W rods and wires along the axial direction, especially at low temperatures, could be improved by the fiber-like structure with elongated grains produced by the increase in the reduction ratio [49, 50]. Therefore, the improvement of impact properties of pure W and W-1%La₂O₃ rods by decrease in diameter

could be attributed to the improvement of strength and ductility, especially at low temperatures, caused by the particular microstructure with elongated grains. However, the optimization of reduction ratio is essential for the W rods for the PFM applications. Although the PFCs of fusion reactors, such as divertor and blanket, requires enough volume to fabricate them, some W rods with relatively large diameter shows non-uniform microstructure, especially along radial direction [46, 48].

3. Integrated interpretation of Charpy impact properties

3.1 Introduction

According to the Charpy impact properties of W materials (hot-rolled plates, forged round-blanks, and swaged rods) mentioned in the chapter 2 based on the open literatures during recent ten years, the followings are clarified and could be pointed out as issues:

- 1) The Charpy impact properties (DBTT, USE, absorbed energy, and fracture manner) are strongly dependent on the fabrication methods and histories even if their major chemical composition is the same.
- 2) The microstructural anisotropy strongly affects the Charpy impact properties.
- 3) The hot-rolled plates and round-blanks along the L-S direction showed the delamination fracture above DBTT to 1000 °C regardless of the dispersion strengthening and alloying.
- 4) The swaged pure W rods along the L-R direction showed the delamination fracture above DBTT to 800 °C and the ductile fracture above 800 °C. In contrast, the K-doped W and W-1%La₂O₃ show the delamination fracture from DBTT to 1000 °C and show no ductile fracture.
- 5) The effects of K-doping, La₂O₃ particles dispersion, and alloying by Ta, Mo, and V on the Charpy impact properties could not be understood systematically based on the

microstructural viewpoints.

It is well known that the grain refining can cause the improvement of mechanical properties of most metals including W [28, 51] even if their major chemical composition is the same, which can be explained in general by the Hall-Petch law [52, 53]. The grain refining is achieved by the increment of reduction ratio in the rolling, forging, and swaging in general. Therefore, the strong dependence of Charpy impact properties on the fabrication methods and histories might include the effect of grain size and shape. The diameter dependence of impact properties of swaged W rods as-mentioned in the section 2.3 could also involve the grain refining effect.

On the other hand, the K-doping and alloying by Re also induce the grain refining of W even if the reduction ratio is the same [41, 54]. Although the details of grain structure (size and shape etc.) of W materials mentioned in the chapter 2 are not clearly reported, the effects of K-doping, La_2O_3 particles dispersion, and alloying by Ta, Mo, and V would be understood by distinguishing the effects of these individual material modifications (the dispersion strengthening by K-bubbles and La_2O_3 particles at grain boundary and the solid solution strengthening and softening) and the effects of grain structure, which could be changed with those modifications.

Based on these discussions, the effect of grain size on the Charpy impact properties of pure W from different production routes are investigated in the present study for the integrated interpretation of them.

3.2 Experimental procedures

Three kinds of pure W were evaluated in the present study. Information of these materials are summarized in table 1. The first one is a pure W plate with 7 mm thickness

fabricated by powder metallurgy and hot rolling, which is provided by Japanese industries. The second one is a pure W plate with 4 mm thickness fabricated by powder metallurgy and hot rolling, which is provided by European industries (see section 2.1). The third one is a pure W round-blank with 175 mm diameter and 29 mm thickness fabricated by powder metallurgy and forging, which is provided by European industries (see section 2.2). Grain size along thickness (d_s) are 22, 19, and 63 μm for the 7 mm thick plate, 4 mm thick plate, and 29 mm thick round-blank, respectively, which are measured in the present study based on the ASTM E112-85 standard [55] using metallographic images of those materials after electrolytic polishing as shown in Fig. 3 (a).

Specimen and methods of the instrumented Charpy impact testing in the present study are based on the EU standards DIN EN ISO 14556:2017-05 [56]. Specimen is a KLST type V-notched one, which has 27 mm length, 3 mm width, and 4 mm thickness. The depth and root radius of the notch are 1 mm and 0.1 mm, respectively. To evaluate the effect of V-notch on Charpy impact properties, an un-notched specimen with 27 mm length, 3 mm width, and 3 mm thickness are also examined (see a photo in Fig. 7). Span of the lower-die of this testing machine is 22 mm for all the tests.

To obtain stable test results, fabrication conditions of the V-notch are considered. Fig. 4 shows cross-sectional metallographic images of notch region of KLST specimen made of the as-received pure W plate with 7 mm thickness. Smooth surface with no scratch is obtained after the optimization of fabrication conditions, as shown in Fig. 4 (c) and (d). No significant difference is observed between the notch surfaces fabricated by diamond grinding (DG) and electrical discharge machining (EDM), as shown in Fig. 4 (a) and (b). Therefore, specimens fabricated by the EDM under the optimized conditions are applied in the present study.

3.3 Results

Test temperature dependences of absorbed energy of Charpy impact tests of KLST specimens along the L-S direction made of the as-received pure W plate with 7 mm thickness, as-received pure W plate with 4 mm thickness [21–25], and as-received pure W round-blank with 175 mm diameter and 29 mm thickness [24, 26] are shown in Fig. 5. The DBTT and USE are varied widely with materials. The DBTTs of 7 mm thick plate, 4 mm thick plate, and 29 mm thick round-blank are approximately 550 °C, 450 °C, and 710 °C, respectively. The USEs, which are the average values of absorbed energy from the DBTT to 1000 °C, of 7 mm thick plate, 4 mm thick plate, and 29 mm thick round-blank are approximately 5.5 J, 6.8 J, and 4.0 J, respectively. These varied values of impact properties might be attributed to the individual particular microstructure dependent on the fabrication methods and histories. As shown in Fig. 6, a linear relation is obtained between these DBTTs and USEs. In this figure, the error bars of USEs mean the difference of the maximum and minimum absorbed energies from the USE.

Appearance of KLST specimens after the impact tests made of the as-received pure W plate with 7 mm thickness are shown in Fig. 7 (a). Below the DBTT (approximately 550 °C), a brittle fracture and a mixture of brittle and delamination fractures are observed at the test temperatures of 400 °C and 500 °C, respectively. In contrast, the delamination fracture is observed at all the test temperatures above the DBTT. These fracture manners observed in this plate with 7 mm thickness of the present study are similar to those observed in the plate with 4 mm thickness [21–25] and round-blank with 175 mm diameter and 29 mm thickness [24, 26].

Test temperature dependences of absorbed energy of Charpy impact tests of un-notched specimens (3 mm x 3 mm x 27 mm) along the L-S direction made of the as-received pure W plate with 7 mm thickness and the appearance of those specimens after

the impact tests are shown in Fig. 8 and Fig. 7 (b), respectively. The DBTT of un-notched specimen is approximately 500 °C, which could be recognized as the same value as that of the V-notched KLST specimen (DBTT \approx 550 °C). Below the DBTT, the un-notched specimen showed the brittle fracture as the V-notched specimen tested at 400 °C showed. In contrast, a plastic bending with no cracks and no fracture surfaces are observed at 600 °C and 800 °C in the un-notched specimen, which is completely different fracture manner from the V-notched specimen tested at the same temperatures. In addition, the absorbed energy above DBTT and the USE (approximately 8.7 J) of the un-notched specimen are approximately 30% higher than those of the V-notched specimen. According to these test results, the DBTT value under the tests along L-S direction is not affected by the V-notch, while the absorbed energy and fracture manner above DBTT are strongly affected by that. Considering the particular microstructure like “pancake” as shown in Fig. 3, it is possible that the delamination fracture above DBTT is peculiar for the tests along L-S direction.

The effect of notch fabrication method on the absorbed energy and fracture manner above DBTT is evaluated in the present study. Fig. 8 and Fig. 7 (c) show the test temperature dependences of absorbed energy of Charpy impact tests of KLST specimens fabricated by the DG along the L-S direction made of the as-received pure W plate with 7 mm thickness and the appearance of those specimens after the impact tests, respectively. The absorbed energy and fracture manner at 600 °C and 800 °C of specimens fabricated by the DG are the same as those of specimens fabricated by the EDM. Therefore, the effect of notch fabrication method could be negligible.

3.4 Discussion

According to several reports on the effect of grain size on impact properties and fracture toughness of metals, the DBTT can be determined by the grain size (d) and a

Hall-Petch type relation expressed by the following equation can be applied [57–59]:

$$\text{DBTT} = A_{\text{DBTT}} - K_{\text{DBTT}} \cdot d^{-1/2} \quad (1)$$

where A_{DBTT} and K_{DBTT} are constants independent of the grain size. This relation indicates that the grain refining can cause the decrease in DBTT. Although there are very limited examples of application of this relation to W materials, Bonnekoh *et al.* reported that the DBTT of cold-rolled pure W sheets obtained by a fracture toughness tests showed good agreement with this equation except very fine grain material [51].

In the present study, to evaluate the possibility of integrated interpretation of the Charpy impact properties of W materials from different production routes, the Hall-Petch type relation is applied not only to the DBTT (see the equation (1)) but to the USE (see the following equation (2)) obtained by specimen along the L-S direction of pure W materials fabricated by the powder metallurgy and hot rolling, forging, and swaging:

$$\text{USE} = A_{\text{USE}} - K_{\text{USE}} \cdot d^{-1/2} \quad (2)$$

where A_{USE} and K_{USE} are constants independent of the grain size. As a grain size for those relations, the grain size along thickness (d_s) is applied, which means a grain size toward crack propagation. The values of d_s are 22, 19, and 63 μm for the 7 mm thick hot-rolled plate, 4 mm thick hot-rolled plate, and 29 mm thick forged round-blank, respectively. The relationships between d_s and USE and DBTT are shown in Fig. 9. The USEs are the average values of absorbed energy above the DBTT to 1000 °C. The error bars mean the difference of the maximum and minimum absorbed energies from the USE. Although the number of data point is very limited, those equations (1) and (2) are clarified to fit very well to the

experimentally determined DBTT and USE of the hot-rolled plates and forged round-blank as a consequence. Therefore, in case of the pure W materials by powder metallurgy, it is possible that the DBTT and USE under the Charpy impact tests could be integrately understood using Hall-Petch type relations even if these materials are from different production routes. As a future work, validity of those relations to the other pure W materials (cold-rolled, warm-rolled, and swaged materials by powder metallurgy and materials by mechanical alloying (MA) and hot isostatic pressing (HIP) etc.) and modified W materials (dispersion-strengthened materials and solid solution strengthened alloys) from different production route and with different microstructure will be investigated.

4. Conclusion

The current status of Charpy impact properties of W materials for the PFM applications below 1000 °C, including pure and modified ones fabricated by several methods and histories, are reviewed based on the open literatures during recent ten years and the possibility of integrated interpretation of Charpy impact properties of W materials from different production routes are discussed. The results of this study are summarized as follows:

- (1) The Charpy impact properties (DBTT, USE, absorbed energy, and fracture manner) are strongly dependent on the fabrication methods and histories even if their major chemical composition is the same.
- (2) The microstructural anisotropy strongly affects the Charpy impact properties. In case of the hot-rolled plates and forged round-blanks, the impact properties along L-S and T-L (S-L) directions are the best and the worst, respectively.
- (3) A brittle fracture below DBTT and a delamination fracture above DBTT to 1000 °C are observed in most of the W materials. The pure W swaged rod only showed a ductile

fracture above 800 °C to 1000 °C, which induces the highest absorbed energy among all W materials evaluated in the present study.

- (4) The effects of dispersion strengthening (K-doping and La₂O₃ particles dispersion) and solid solution strengthening and softening (alloying by Ta, Mo, and V) on the Charpy impact properties could not be clearly understood based on the microstructural viewpoints.
- (5) In case of the pure W materials by powder metallurgy, it is possible that the DBTT and USE under the Charpy impact tests could be integrately understood using Hall-Petch type relations ($DBTT, USE = A - K \cdot d^{-1/2}$, where A and K are constants independent of the grain size) even if these materials are from different production routes.

Acknowledgement

This work was supported by JSPS KAKENHI Grant Number 15KK0224 and 26289351. Authors are grateful to the staff of Miyakojima Seisakusho Co. Ltd. for their optimization of the fabrication process of the Charpy impact test specimens.

References

- [1] R. Toschi, P. Barabaschi, D. Campbell, F. Elio, D. Maisonnier, D. Ward, *Fusion Eng. Des.* **56–57** (2001) 163–172.
- [2] S. Wurster, N. Baluc, M. Battabyal, T. Crosby, J. Du, C. García-Rosales, A. Hasegawa, A. Hoffmann, A. Kimura, H. Kurishita, R.J. Kurtz, H. Li, S. Noh, J. Reiser, J. Riesch, M. Rieth, W. Setyawan, M. Walter, J.-H. You, R. Pippan, *J. Nucl. Mater.* **442** (2013) S181–S189.
- [3] P. Gumbsch, *J. Nucl. Mater.* **323** (2003) 304–312.
- [4] M. Faleschini, H. Kreuzer, D. Kiener, R. Pippan, *J. Nucl. Mater.* **367–370** (2007) 800–805.
- [5] A. Giannattasio, M. Tanaka, T. D. Joseph, S. G. Roberts, *Phys. Scr.* **T128** (2007) 87–90.
- [6] A. Giannattasio, S. G. Roberts, *Phil. Mag.* **Vol. 87, No. 17** (2007) 2589–2598.
- [7] D. Rupp, S. M. Weygand, *J. Nucl. Mater.* **386–388** (2009) 591–593.
- [8] D. Rupp, R. Mönig, P. Gruber, S. M. Weygand, *Int. J. Refract. Met. Hard Mater.* **28** (2010) 669–673.
- [9] D. Rupp, S. M. Weygand, *Phil. Mag.* **Vol. 90, No. 30**, (2010) 4055–4069.
- [10] D. Rupp, S. M. Weygand, *J. Nucl. Mater.* **417** (2011) 477–480.
- [11] E. Gaganidze, D. Rupp, J. Aktaa, *J. Nucl. Mater.* **446** (2014) 240–245.
- [12] A.V. Babak, *Strength of Materials* **14** (1982) 1389–1391.
- [13] N.D. Bega, A.V. Babak, E.I. Uskov *Soviet Powder Metallurgy and Metal Ceramics* **21** (1982) 408–411.
- [14] A.V. Babak, *Soviet Powder Metallurgy and Metal Ceramics* **22** (1983) 316–318.
- [15] A.V. Babak, E.I. Uskov, *Strength of Materials* **15** (1983) 667–672.
- [16] I. Uytendhouwen, R. Chaouadi, J. Linke, V. Massaut, G. Van Oost, *Advanced Materials* **59** (2008) 319–325.

- [17] M. Wirtz, J. Linke, Th. Loewenhoff, G. Pintsuk, I. Uytendhouwen, *Phys. Scr.* **T167** (2016) 014015.
- [18] M. Fukuda, S. Nogami, K. Yabuuchi, A. Hasegawa, T. Muroga, *Fus. Sci. Tech.* **68** (2015) 690–693.
- [19] W. H. Guan, S. Nogami, M. Fukuda, A. Sakata, A. Hasegawa, *Plasma Fus. Res.* **10** (2015) 1405073-1–1405073-10.
- [20] S. Nogami, W. H. Guan, M. Fukuda, A. Hasegawa, *Fus. Eng. Des.* **109–111** (2016) 1549–1553.
- [21] M. Rieth, A. Hoffmann, *Int. J. Refract. Met. Hard Mater.* **28** (2010) 679–686.
- [22] J. Reiser, M. Rieth, B. Dafferner, A. Hoffmann, *J. Nucl. Mater.* **442** (2013) S204–S207.
- [23] J. Reiser, L. Garrison, H. Greuner, J. Hoffmann, T. Weingärtner, Ute Jäntschi, M. Klimenkov, P. Franke, S. Bonk, C. Bonnekoh, S. Sickinger, S. Baumgärtner, D. Bolich, M. Hoffmann, R. Ziegler, J. Konrad, J. Hohe, A. Hoffmann, T. Mrotzek, M. Seiss, M. Rieth, A. Möslang, *Int. J. Refract. Met. Hard Mater.* **69** (2017) 66–109.
- [24] M. Rieth, D. Armstrong, B. Dafferner, S. Heger, A. Hoffmann, M.-D. Hoffmann, U. Jäntschi, C. Kübel, E. Materna-Morris, J. Reiser, M. Rohde, T. Scherer, V. Widak, H. Zimmermann, *Advances in Science and Technology* **73** (2010) 11–21.
- [25] M. Rieth, A. Hoffmann, *Advances in Science and Technology* **59** (2008) 101–104.
- [26] M. Rieth, J. Reiser, B. Dafferner, S. Baumgärtner, *Fus. Sci. Technol.* **61** (2012) 381–384.
- [27] T. Hirai, F. Escourbiac, V. Barabash, A. Durocher, A. Fedosov, L. Ferrand, T. Jokinen, V. Komarov, M. Merola, S. Carpentier-Chouchana, N. Arkhipov, V. Kuznetsov, A. Volodin, S. Suzuki, K. Ezato, Y. Seki, B. Riccardi, M. Bednarek, P. Gavila, *J. Nucl. Mater.* **463** (2015) 1248–1251.
- [28] K. Farrell, A. C. Schaffhauser, J. O. Stiegler, *J. Less-Common Met.* **13** (1967) 141–155.
- [29] Q. Wei and L.J. Kecskes, *Mater. Sci. Eng. A* **491** (2008) 62–69.

- [30] A. Luo, K. S. Shin, D. L. Jacobson, *Scr. Metall.* **25** (1991) 2411–2414.
- [31] P. Makarov and K. Povarova, *Int. J. Refract. Met. Hard Mater.* **20** (2002) 277–285.
- [32] J. W. Pugh, *Metall. Trans. A* **4** (1973) 533–538.
- [33] P. K. Wright, *Metall. Trans. A* **9** (1978) 955–963.
- [34] D. B. Snow, *Metall. Trans. A* **10** (1979) 815–821.
- [35] P. Schade, *Int. J. Refract. Met. Hard Mater.* **28** (2010) 648–660.
- [36] J. Martínez, B. Savoini, M. A. Monge, A. Muñoz, R. Pareja, *Fus. Eng. Des.* **86** (2011) 2534–2537.
- [37] A. Patra, R. R. Sahoo, S. K. Karak, S. K. Sahoo, *J. Refract. Met. Hard Mater.* **70** (2018) 134–154.
- [38] H. Kurishita, S. Kobayashi, K. Nakai, T. Ogawa, A. Hasegawa, K. Abe, H. Arakawa, S. Matsuo, T. Takida, K. Takebe, M. Kawai, N. Yoshida, *J. Nucl. Mater.* **377** (2008) 34–40.
- [39] W. H. Guan, S. Nogami, M. Fukuda, A. Hasegawa, *Fus. Eng. Des.* **109–111** (2016) 1538–1542.
- [40] S. Nogami, W. H. Guan, A. Hasegawa, M. Fukuda, *Fus. Sci. Tech.* **72** (2017) 673–679.
- [41] A. Hasegawa, M. Fukuda, T. Tanno, S. Nogami, K. Yabuuchi, T. Tanaka, T. Muroga, *Proc. of 25th IAEA Fusion Energy Conference, MPT02*, (2014).
- [42] K. Sasaki, K. Yabuuchi, S. Nogami, A. Hasegawa, *J. Nucl. Mater.* **461** (2015) 357–364.
- [43] W. D. Klopp, *J. Less-common Met.* **42** (1975) 261–278.
- [44] J. L. Taylor, *J. Less-common Met.* **7** (1964) 278–287.
- [45] P. L. Raffo, *J. Less-common Met.* **17** (1969) 133–149.
- [46] G. Pintsuk and I. Uytendhouwen, *Int. J. Refract. Met. Hard Mater.* **28** (2010) 661–668.
- [47] H. Sheng, I. Uytendhouwen, G. V. Oost, J. Vleugels, *Nucl. Eng. Des.* **246** (2012) 198–202.
- [48] W. H. Guan, S. Nogami, M. Fukuda, A. Hasegawa, *Fus. Eng. Des.* **109–111** (2016)

1538–1542.

[49] D. Lee, *Metall. Trans. A* **6** (1975) 2083–2088.

[50] J. F. Peck, D. A. Thomas, *Trans. Metall. Soc. AIME*, **221** (1961) 1240–1246.

[51] C. Bonnekoh, A. Hoffmann, J. Reiser, *Int. J. Refract. Met. Hard Mater.* **71** (2018) 181–189.

[52] E. O. Hall, *Proc. Phys. Soc. London Sect. B* **64** (1951) 747–753.

[53] N. J. Petch, *J. Iron Steel Inst., London* **173** (1953) 25–28.

[54] K. Tsuchida, T. Miyazawa, A. Hasegawa, S. Nogami, M. Fukuda, *Nucl. Mater. Energy* **15** (2018) 158–163.

[55] ASTM E112–85, Standard Methods for Determining the Average Grain Size, *Annual Book of ASTM*, 1986, 227–290.

[56] DIN EN ISO 14556:2017-05, *Metallische Werkstoffe - Kerbschlagbiegeversuch nach Charpy (V-Kerb) - Instrumentiertes Prüfverfahren (ISO 14556:2015); Deutsche Fassung EN ISO 14556:2015 [in German]*.

[57] N. J. Petch, *Philos. Mag.* **3** (1958) 1089.

[58] A. N. Stroh, *Adv. Phys.* **6** (1957) 48.

[59] T. Hanamura, F. Yin, K. Nagai, *ISIJ Int.* **44** (2004) 610–617.

Table 1 Information of pure W materials used and referred in the present study.

Form	Material		Grain size along thickness, d_s [μm]	Remarks
	Method	Size [mm] *		
Plate	Hot-rolling	t7	22	
Plate	Hot-rolling	t4	19	Charpy impact test data were obtained from ref. 21–25.
Round-blank	Forging	$\phi 175 \times t29$	63	Charpy impact test data were obtained from ref. 24 and 26.

* t4, t7, and t29 mean 4 mm, 7 mm, and 29 mm in thickness, respectively. $\phi 175$ means 175 mm in diameter.

Fig. 1 Test temperature dependences of absorbed energy of Charpy impact tests of KLST specimens made of as-received W materials. (a) hot-rolled plates with 4 mm thickness made of pure W (L-S, L-T, and T-L directions), K-doped W (L-T, and T-L directions), and W-1%La₂O₃ (L-T, and T-L directions) [21–25]. (b) forged round-blanks with 175 mm diameter and 29 mm thickness made of pure W (L-S, L-T, and S-L directions), W-1%Ta (L-S direction), W-5%Ta (L-S direction), W-20%Mo (L-T direction), W-50%Mo (L-T direction), and W-5%V (L-T direction) [24, 26]. (c) swaged rods (L-R direction) made of pure W with 6.9 and 20 mm diameters, K-doped W with 6.9 mm diameter, W-1%La₂O₃ with 6.9 and 16 mm diameters, and W-1%Re-1%La₂O₃ with 10 mm diameter [21, 24–26].

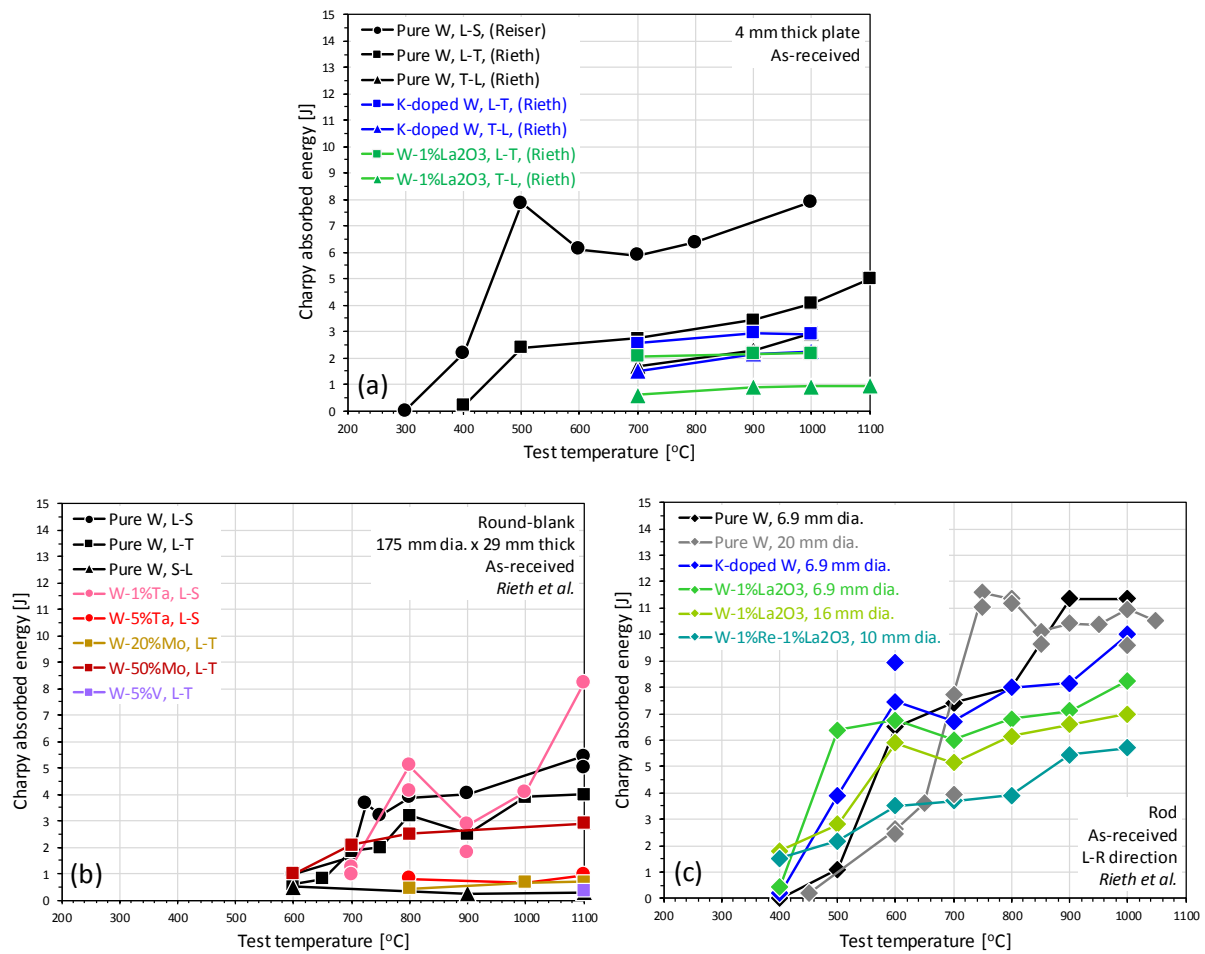


Fig. 2 Nomenclature of directions of materials and KLST specimen. (a) hot-rolled plate, (b) forged round-blank, and (c) swaged rod.

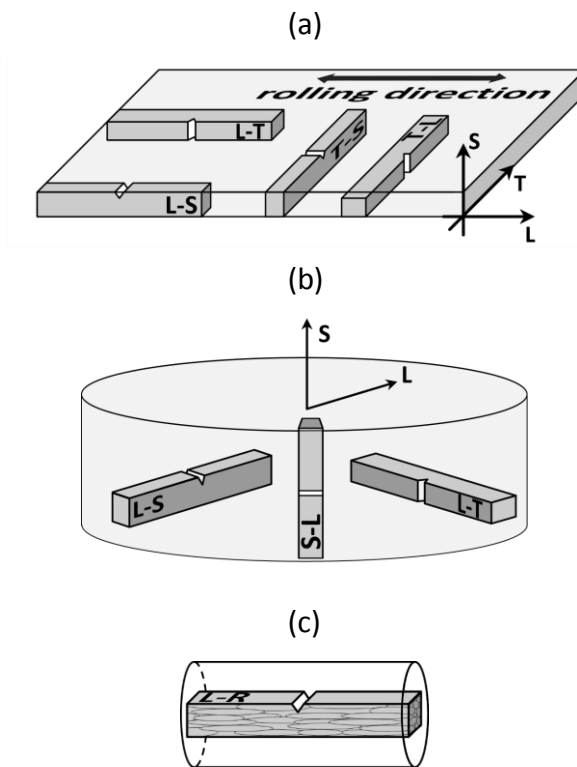


Fig. 3 (a) 3D metallographic image after electrolytic polishing and (b) 3D inverse pole figure (IPF) image obtained by electron backscatter diffraction (EBSD) analysis of as-received pure W plate (t7 mm).

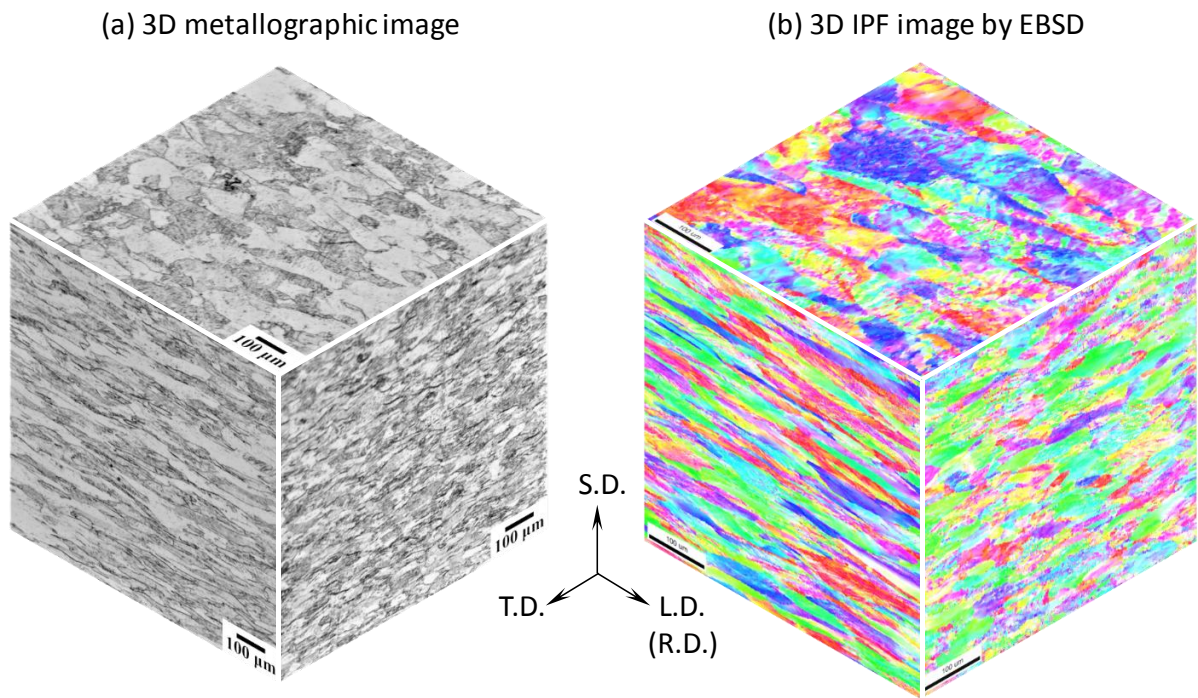


Fig. 4 Cross-sectional metallographic images of notch region of KLST specimen (as-received pure W plate (t7 mm)) fabricated (a) by diamond grinding (DG) and (b–d) by electrical discharge machining (EDM). (c) and (d) are typical images before and after the optimization.

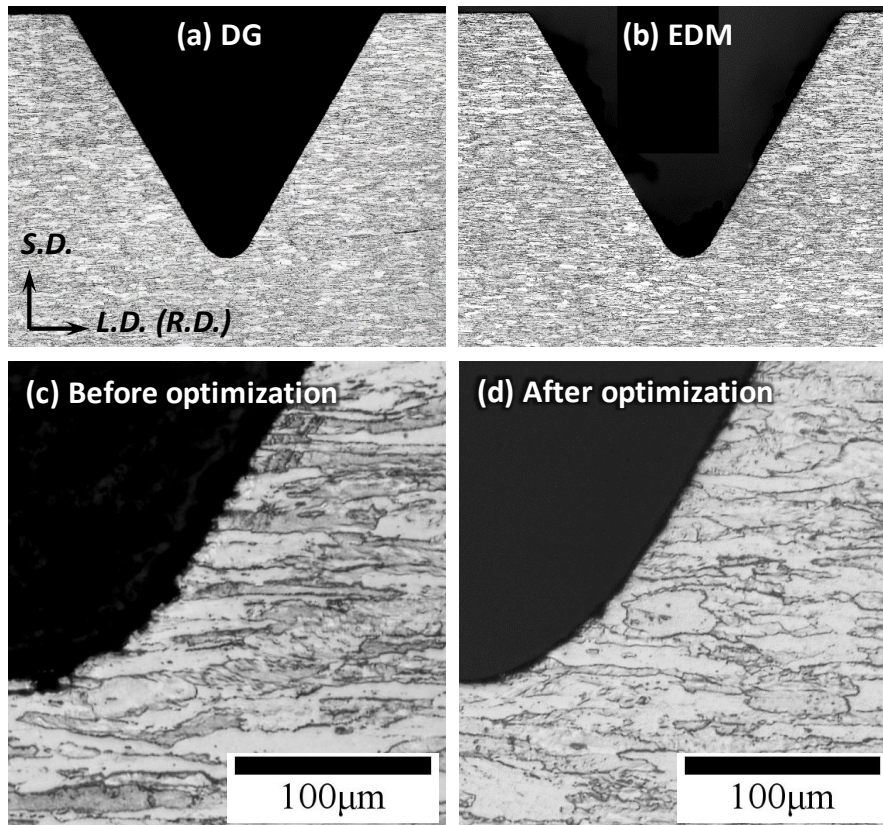


Fig. 5 Test temperature dependences of absorbed energy of Charpy impact tests of KLST specimens (L-S direction) made of as-received pure W plate (t7 mm), as-received pure W plate (t4 mm) [21–25], and as-received pure W round-blank (ϕ 175 mm x t29 mm) [24, 26].

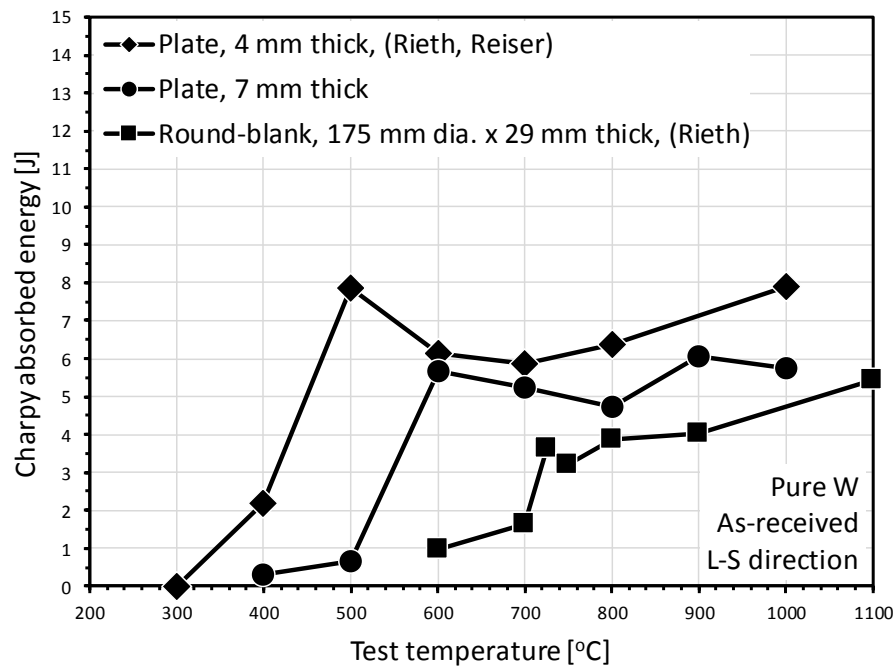


Fig. 6 Relationship between USE and DBTT obtained by Charpy impact tests of KLST specimens (L-S direction) made of as-received pure W plate (t7 mm), as-received pure W plate (t4 mm) [21–25], and as-received pure W round-blank (ϕ 175 mm x t29 mm) [24, 26]. The USEs are the average values of absorbed energy above the DBTT to 1000 °C.

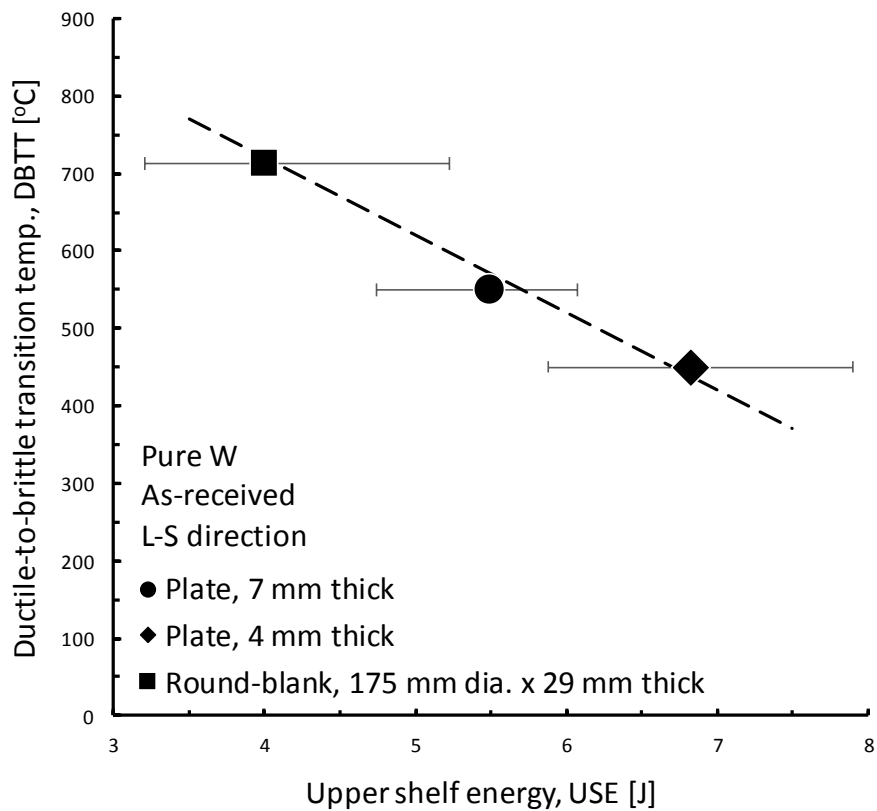



Fig. 7 Appearance of specimens after Charpy impact tests (L-S direction) made of pure W plate (t7 mm, as-received). (a) KLST specimen (3 mm x 4 mm x 27 mm) fabricated by electro discharge machining (EDM), (b) un-notched specimen (3 mm x 3 mm x 27 mm) fabricated by EDM, and (c) KLST specimen fabricated by diamond grinding (DG). Descriptions in the right column for each specimen indicate fracture manner.

(a) KLST specimen (3 x 4 x 27 mm ³) by EDM		(b) Un-notched specimen (3 x 3 x 27 mm ³) by EDM		(c) KLST specimen (3 x 4 x 27 mm ³) by DG	
	Del.				
	Del.				
	Del.		Duc.		Del.
	Del.				
	Del.		Duc.		Del.
	Bri. + Del.				
	Bri.		Bri.		

* Duc.:Ductile fracture, Del.: Delamination, Bri.: Brittle fracture

Fig. 8 Test temperature dependences of absorbed energy of Charpy impact tests of three kinds of specimens along L-S direction made of pure W plate (t7 mm, as-received). The first specimen is notched KLST specimen (3 mm x 4 mm x 27 mm) fabricated by electro discharge machining (EDM), the second one is un-notched specimen (3 mm x 3 mm x 27 mm) fabricated by EDM, and the third one is notched KLST specimen fabricated by diamond grinding (DG).

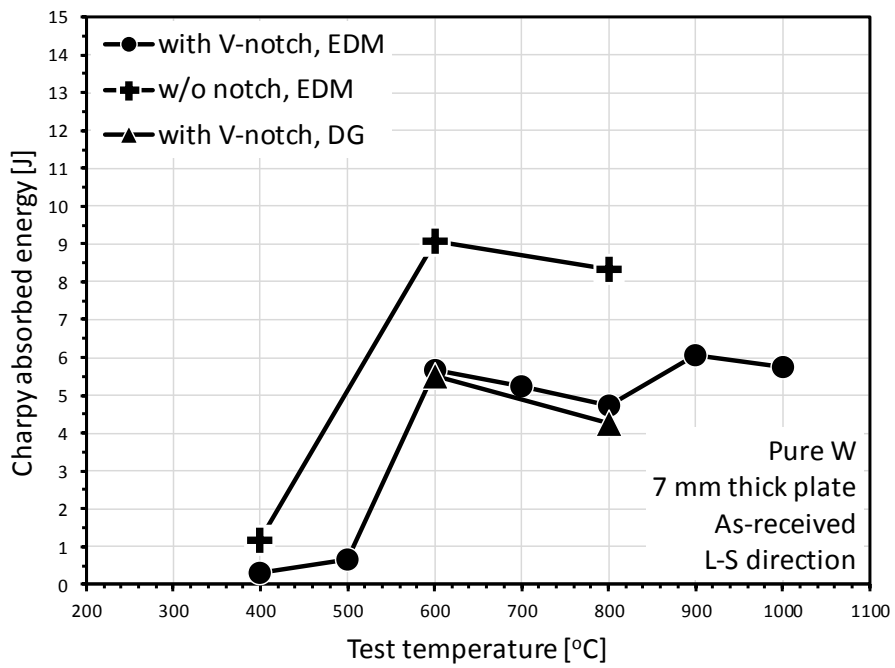


Fig. 9 Relationship between grain size along thickness (d_s) and USE and DBTT obtained by Charpy impact tests of KLST specimens (L-S direction) made of as-received pure W plate (t7 mm), as-received pure W plate (t4 mm) [21–25], and as-received pure W round-blank (ϕ 175 mm x t29 mm) [24, 26]. The USEs are the average values of absorbed energy above the DBTT to 1000 °C.

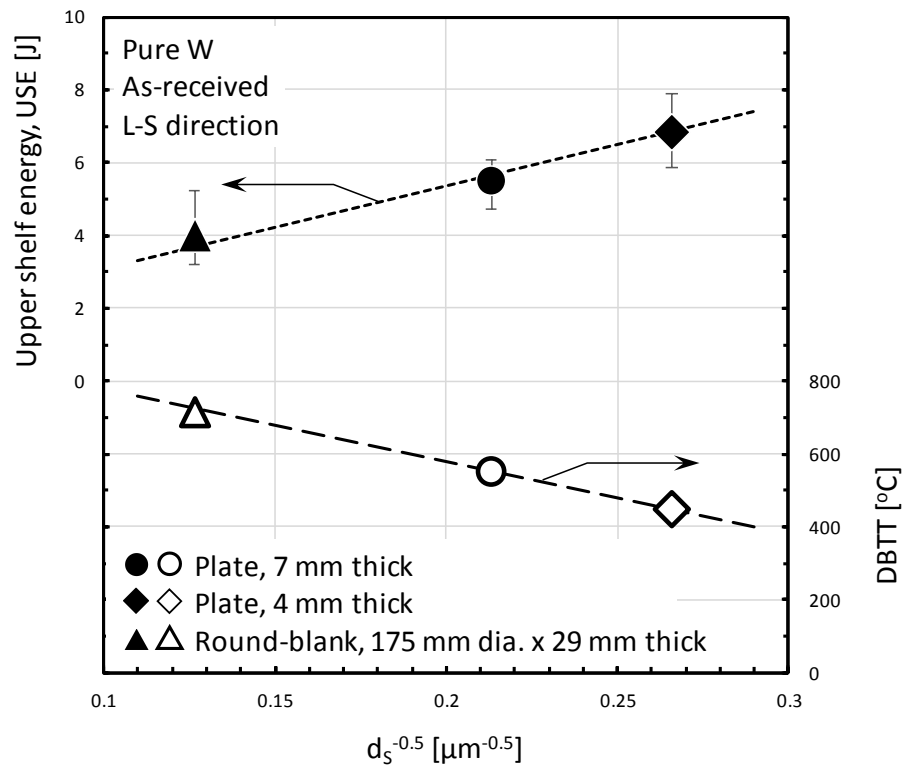


Figure 1 Test temperature dependences of absorbed energy of Charpy impact tests of KLST specimens made of as-received W materials.

(a) hot-rolled plates with 4 mm thickness made of pure W (L-S, L-T, and T-L directions), K-doped W (L-T, and T-L directions), and W-1%La₂O₃ (L-T, and T-L directions).

(b) forged round-blanks with 175 mm diameter and 29 mm thickness made of pure W (L-S, L-T, and S-L directions), W-1%Ta (L-S direction), W-5%Ta (L-S direction), W-20%Mo (L-T direction), W-50%Mo (L-T direction), and W-5%V (L-T direction).

(c) swaged rods (L-R direction) made of pure W with 6.9 and 20 mm diameters, K-doped W with 6.9 mm diameter, W-1%La₂O₃ with 6.9 and 16 mm diameters, and W-1%Re-1%La₂O₃ with 10 mm diameter.

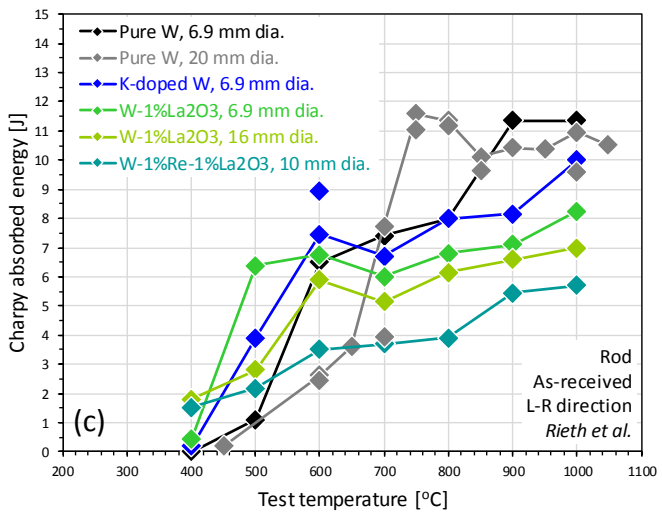
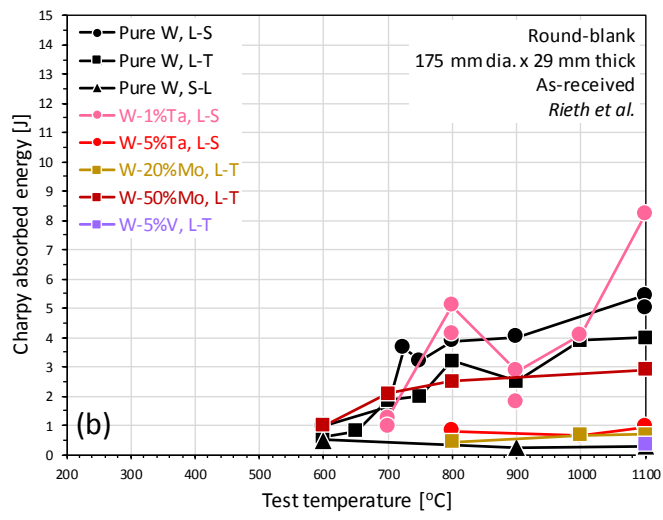
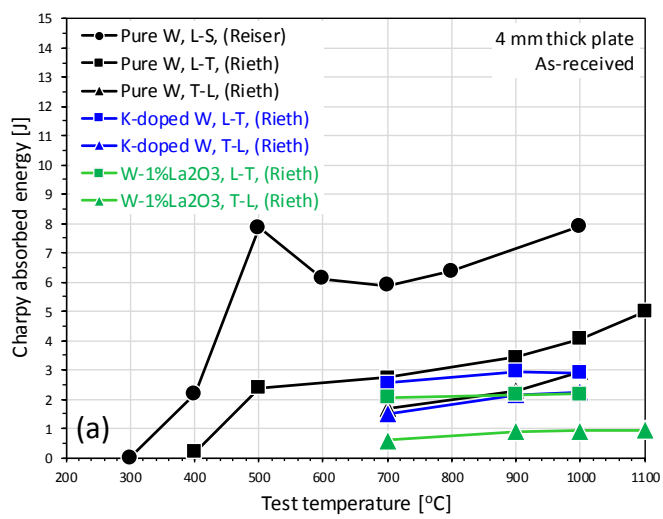


Fig. 2 Nomenclature of directions of materials and KLST specimen. (a) hot-rolled plate, (b) forged round-blank, and (c) swaged rod.

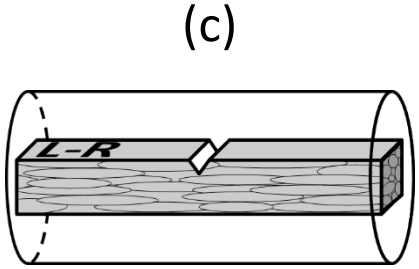
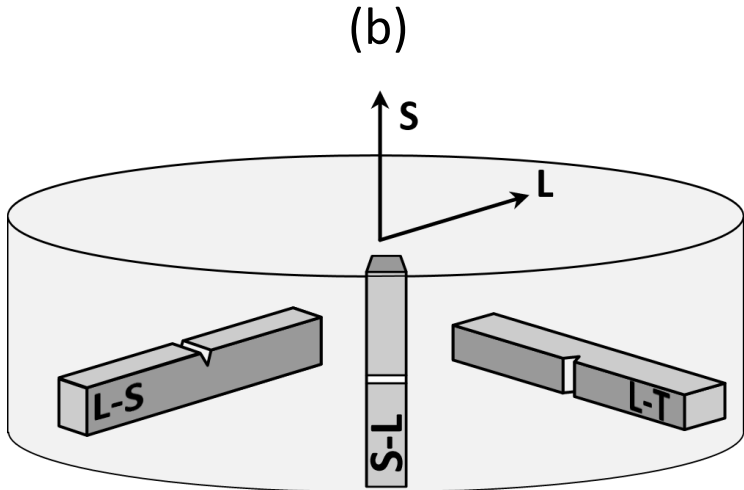
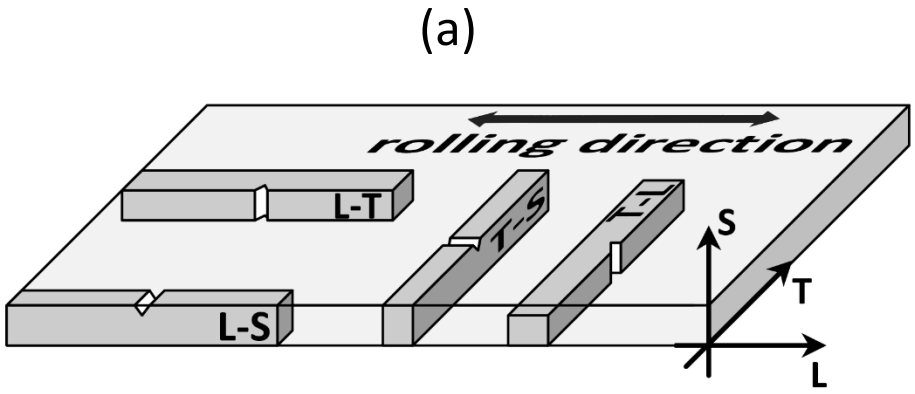
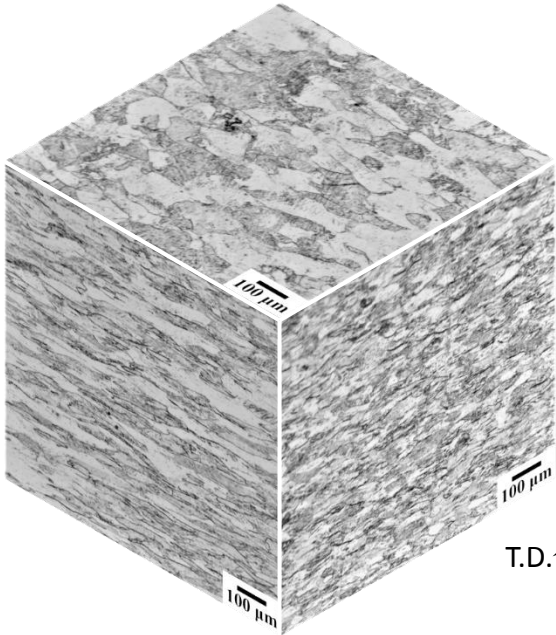


Fig. 3 (a) 3D metallographic image after electrolytic polishing and (b) 3D inverse pole figure (IPF) image obtained by electron backscatter diffraction (EBSD) analysis of as-received pure W plate (t7 mm).

(a) 3D metallographic image



(b) 3D IPF image by EBSD

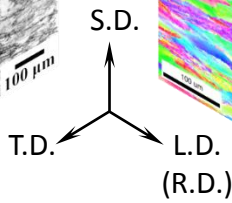
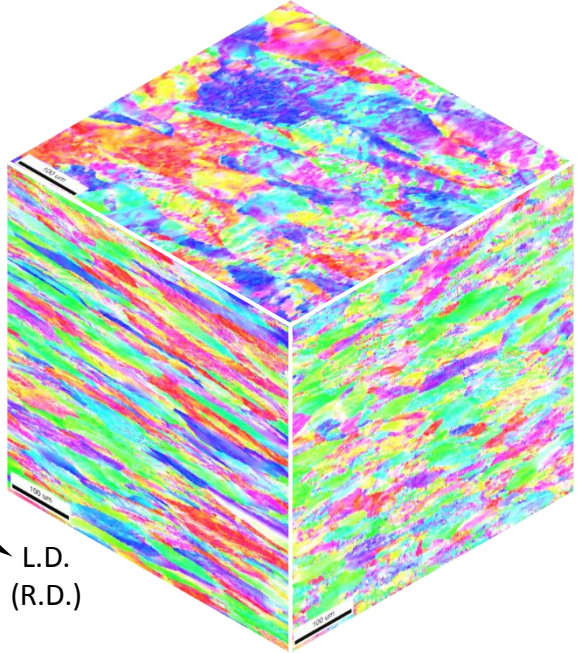


Fig. 4 Cross-sectional metallographic images of notch region of KLST specimen (as-received pure W plate (t7 mm)) fabricated (a) by diamond grinding (DG) and (b-d) by electrical discharge machining (EDM). (c) and (d) are typical images before and after the optimization.

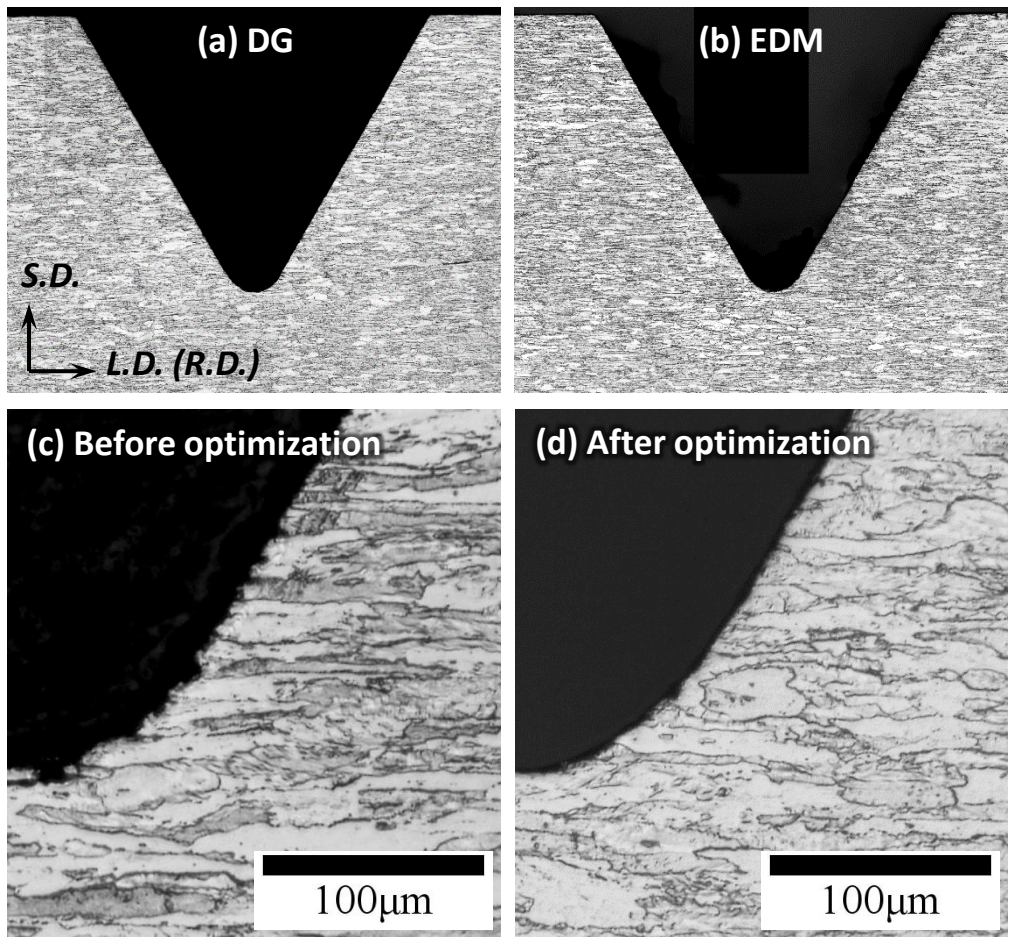


Fig. 5 Test temperature dependences of absorbed energy of Charpy impact tests of KLST specimens (L-S direction) made of as-received pure W plate (t7 mm), as-received pure W plate (t4 mm) [21–25], and as-received pure W round-blank (ϕ 175 mm x t29 mm) [24, 26].

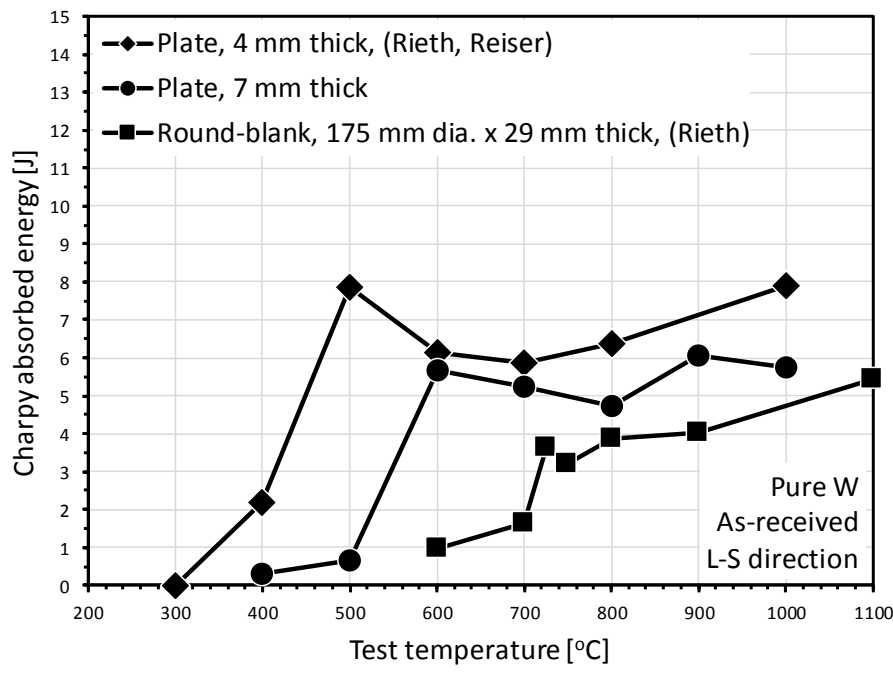


Fig. 6 Relationship between USE and DBTT obtained by Charpy impact tests of KLST specimens (L-S direction) made of as-received pure W plate (t7 mm), as-received pure W plate (t4 mm) [21–25], and as-received pure W round-blank (ϕ 175 mm x t29 mm) [24, 26]. Upper shelf energy values are the average values of absorbed energy above the DBTT and below 1000 ° C.

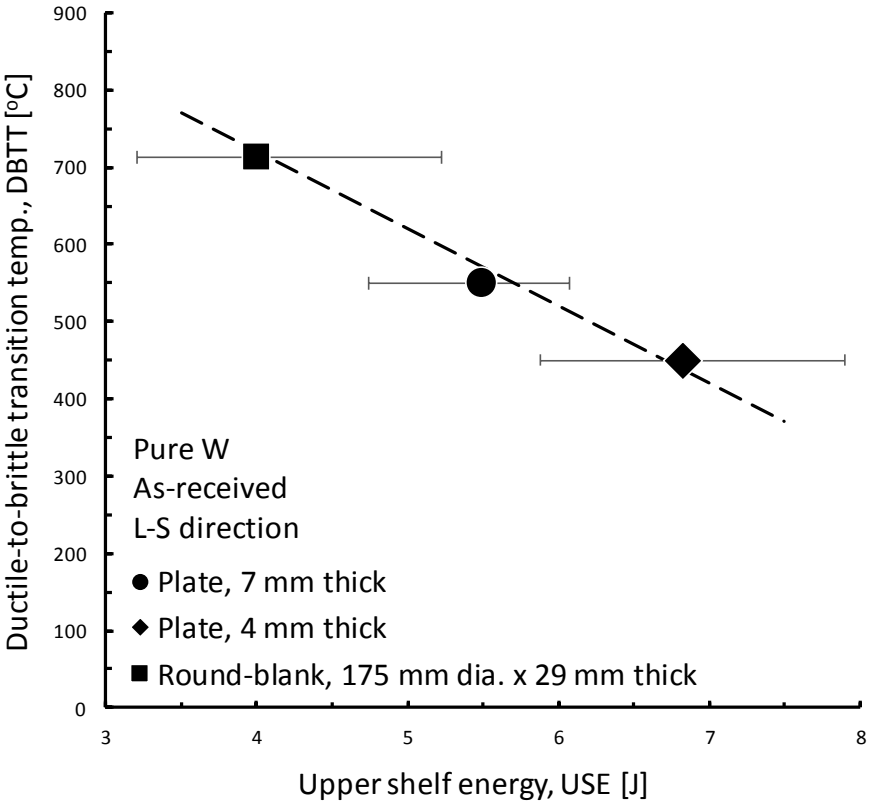


Fig. 7 Appearance of specimens after Charpy impact tests (L-S direction) made of pure W plate (t7 mm, as-received). (a) KLST specimen (3 mm x 4 mm x 27 mm) fabricated by electro discharge machining (EDM), (b) un-notched specimen (3 mm x 3 mm x 27 mm) fabricated by EDM, and (c) KLST specimen fabricated by diamond grinding (DG). Descriptions in the right column for each specimen show fracture manner.

(a) KLST specimen (3 x 4 x 27 mm ³) by EDM		(b) Un-notched specimen (3 x 3 x 27 mm ³) by EDM		(c) KLST specimen (3 x 4 x 27 mm ³) by DG	
1000 °C 	Del.	 Notched Un-notched			
900 °C 	Del.				
800 °C 	Del.	800 °C 	Duc.	800 °C 	Del.
700 °C 	Del.				
600 °C 	Del.	600 °C 	Duc.	600 °C 	Del.
500 °C 	Bri. + Del.				
400 °C 	Bri.	400 °C 	Bri.		

* Duc.:Ductile fracture, Del.: Delamination, Bri.: Brittle fracture

Fig. 8 Test temperature dependences of absorbed energy of Charpy impact tests of three kinds of specimens along L-S direction made of pure W plate (t7 mm, as-received). The first specimen is notched KLST specimen (3 mm x 4 mm x 27 mm) fabricated by electro discharge machining (EDM), the second one is un-notched specimen (3 mm x 3 mm x 27 mm) fabricated by EDM, and the third one is notched KLST specimen fabricated by diamond grinding (DG).

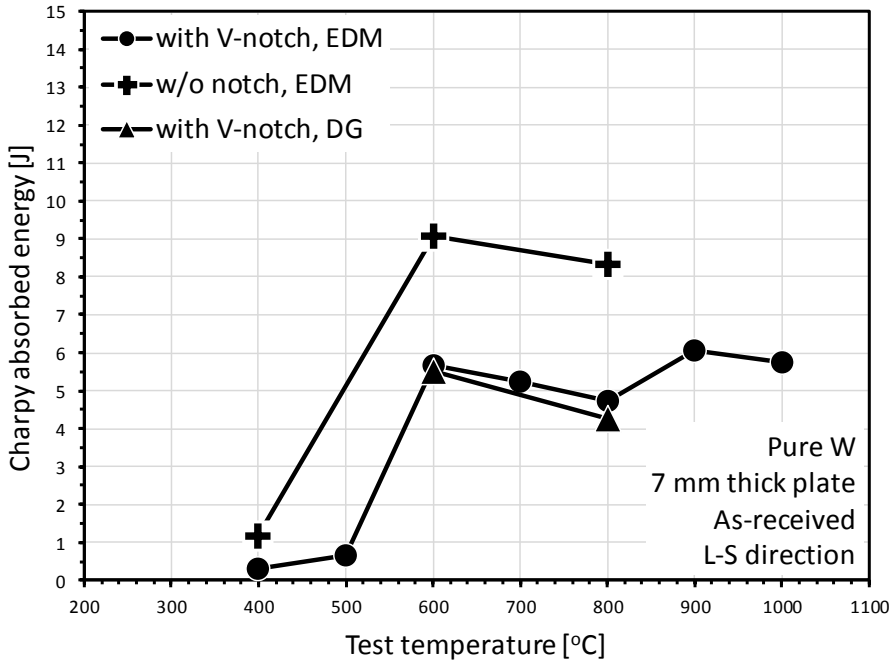


Fig. 9 Relationship between grain size along thickness (d_s) and USE and DBTT obtained by Charpy impact tests of KLST specimens (L-S direction) made of as-received pure W plate (t7 mm), as-received pure W plate (t4 mm) [21–25], and as-received pure W round-blank ($\phi 175$ mm x t29 mm) [24, 26]. Upper shelf energy values are the average values of absorbed energy above the DBTT and below 1000 ° C.

